

TIANJIN INSAR TIME SERIES ANALYSIS WITH L- AND X-BAND

*Qingli Luo¹, Daniele Perissin^{*1}, Qinghua Li¹, Hui Lin¹, and Ralf Duering²*

(¹ISEIS, Chinese University of Hong Kong, Hong Kong SAR, China;
²Infoterra, Germany)

ABSTRACT

TerraSAR X-band provides high resolution of 1m, short revisit period of 11days, and sensitive subsidence information, while it cannot afford relatively so high temporal and spatial coherence and wide area coverage as ALOS L-band data. In this work, we exploited the potential of combining L- and X-band for subsidence monitoring. A case study was conducted in Tianjin induced by water withdrawal. A total of 9 ALOS images acquired from 2009/4/24 to 2010/10/28 and 37 TerraSAR-X images acquired from 2009/4/29 to 2010/11/11 were used in INSAR time series analysis for retrieving subsidence in the study area. DINSAR analysis based on Minimum Spanning Tree(MST) was applied into L-band to identify potential deformation area and X-band Permanent Scatterers (PS) analysis for this area was carried out for subsidence time series study.

Index Terms— Tianjin, L- and X-band, subsidence, INSAR

1. INTRODUCTION

Ground subsidence becomes a world problem and China bears remarkable costs caused by subsidence [1]. With the development of local industry and urbanization, excessive ground water withdrawal urges Tianjin to be one of the major subsidence regions in China [2, 3]. Great effort has been made for exploring an effective way to monitor subsidence [4]. Traditional techniques depending on leveling and Global Positioning System (GPS) [5-8] need fixed network stations, a great deal of manpower, and long time span. Differential Interferometric Synthetic Aperture Radar (DINSAR) has been widely applied in subsidence monitoring with its all-time, all-weather and wide area monitoring ability [9, 10]. In order to avoid the limitation of temporal and spatial decorrelation and atmospheric disturbance, Permanent Scatterers (PS) technology [11, 12] was developed as a powerful tool for subsidence monitoring. The main drawback of SAR data has been the poor resolution. However, with the launch of new generation high Resolution SAR satellites, the level of details visible in SAR images increased dramatically [13, 14]. TerraSAR-X

(TSX) and COSMO provide 1m resolution, and Radarsat-II 3m. Meanwhile, the revisit period has been decreased as TSX 11 days, Radarsat-II 24 days. In the case of satellite constellations, COSMO-Skymed provides 1 day interval data. For TSX, it is a new German radar satellite and carries a high frequency X-band (3.1cm). One of the new features is that it can work in Spotlight mode, offering excellent precision for more details in surface observation.

TSX provides high resolution, short revisit period, and sensitive subsidence information, while it cannot afford relatively so good coherence and wide area coverage as ALOS L-band data. The comprehensive utilization of multi-sensor SAR data could provide broader applications and more reliable results for subsidence monitoring. In this paper, we introduce the research carried out at the Institute of Space and Information Science of Hong Kong on the INSAR time series analysis subject. Both L-band and X-band images are exploited to monitor subsidence in Tianjin. L-band wide coverage and high coherence can in fact be exploited to decide the areas where to focus highly dynamic satellites as TSX, with high performances and resolution but less spatial coverage. The output of the work will be useful to drive future acquisition policies of satellites. Moreover, in order to fully consider both temporal and spatial coherence, we developed a multi-temporal DINSAR analysis based on Minimum Spanning Tree (MST) [15], creating a framework for optimal interferometric pairs selection.

2. METHODOLOGY

The strategy we adopted for analyzing this case study can be divided into the following steps: 1) L-Band DInSAR analysis over the whole region. In this way we can exploit the high coherence of L band and the wide coverage to find hot spot areas affected by surface displacement. 2) Once the hot spot areas are identified, we can focus the attention on smaller areas and collect many TSX images, acquired with shorter revisit time. We can then carry out multi-temporal analysis and study the displacement time series.

2.1 L-band DINSAR analysis based on MST algorithm

L-band (23cm wavelength) from ALOS launched by JAXA in January, 2006, supports the relatively high temporal and spatial coherence data with wide-area coverage. For traditional PS technology, the differential interferometric pairs are generated to one common master image. However, DINSAR analysis is affected by temporal and geometric decorrelation. Small Baseline Subset Approach (SBAS) was exploited to reduce only the temporal decorrelation [16, 17]. Then, In order to make full use of temporal and spatial coherence, we construct interferometric pairs by utilizing optimal temporal and spatial coherence among these time series SAR images based on MST algorithm, similarly to what has been done in [15]. It provides a different choice for the selection of interferometric pairs. Then, we can construct several interferometric pairs from available time series SAR images. An extended DEM (SRTM 90m) was applied for the remove of topography phase. After that processing, differential interferograms were generated. From the analysis of these differential interferograms, the potential deformation areas were highlighted.



Figure 1. Spatial coverage of X (blue) and L band (red).

2.2 X-band PS analysis

After the potential deformation areas were identified by L-band DINSAR analysis, we try to apply X-band PS analysis for one of the potential deformation areas. PS technology has been proposed in wide area subsidence monitoring within mm level accuracy and meters of spatial resolution. The core idea is searching for targets (such as buildings, etc.) of relatively stable scattering properties from interferometric pairs a long temporal series of and obtaining reliable deformation and height correction. Due to better resolution, X-band is expected to have the potential ability to monitor subsidence of individual infrastructure including high speed railway as well as urban buildings. The processing steps can be divided into several following major processing steps: SAR data calibration and registration, differential interferogram generation, Permanent Scatterer Candidates(PSC) selection, multi-image sparse grid phase unwrapping, APS estimation and removal, pixel time series analysis and PS points deformation estimation.

3. CASE STUDY

The case study area is located in the west of Tianjin downtown. The center latitude and longitude are 39.11° and 116.85° , respectively. The exploited SAR data set is composed of 8 ALOS images acquired from 2009/4/24 to 2010/10/28 and from 37 TSX images acquired from 2009/4/29 to 2010/11/11. The spatial coverage of L-Band (red rectangle) and X-Band (blue one) are shown in Google earth map as Figure 1. The DINSAR and PS analysis have been carried out using the SARPROZ software [18].

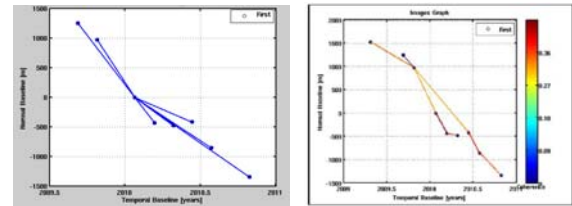
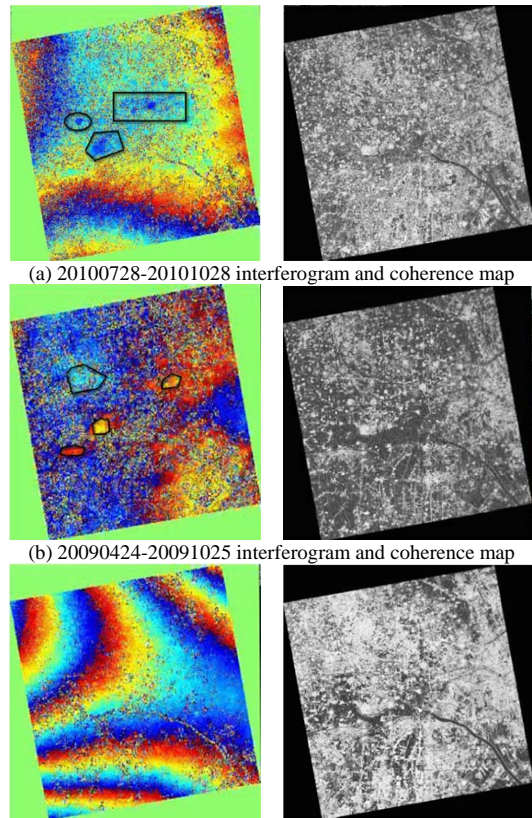


Figure 2. Left: the traditional image graph of ALOS. Right: The image graph based on MST.



(C) 20100312-20100427 interferogram and coherence map
Figure 3. Three selected interferograms of L-band.

We report here the results of L band interferograms generation. Figure 2 shows the L band dataset in the normal-temporal baselines space. In particular two combinations for interferograms generation are shown, the Star Graph (single master) and the MST Graph (the set of most coherent interferograms connecting all available images). Figures 3 show three differential geocoded interferograms taken among those of the MST Graph.

As highlighted with black frames in Figures 3, it is basically possible to detect strong deformation by observing L band interferograms. In the three reported examples, the temporal baselines are respectively 92, 184 and 46 days and the normal baselines 439m, 558m and 41m (height of ambiguity: 130m, 103m and 1400m). As visible from Figure 3(a) and (b) Right, L band shows the expected coherence and allows to easily individuating subsiding areas even in presence of strong atmospheric disturbances, as the Figure 3(a) and (b) Left shows. However, there are some interferograms affected by atmospheric disturbance and the deformation information cannot be easily detected from the single interferogram as the Figure 3(c) Left, even if the coherence map is as good as Figure 3(c) Right shows. Based on the reported analysis, we processed extracting areas that show strong motion in order to examine them with X band data.

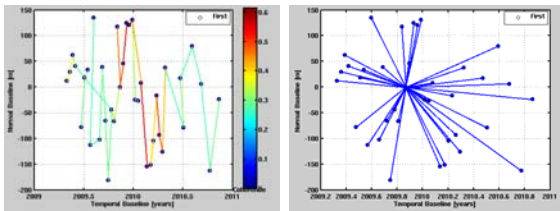


Figure 4. Left: The image graph of TSX based on MST. Right: the traditional image graph.

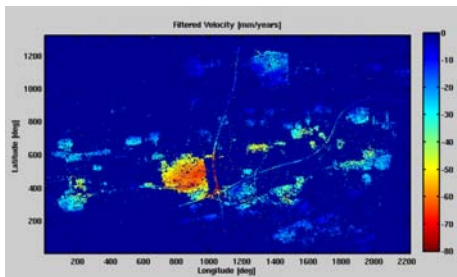


Figure 5. The average motion map



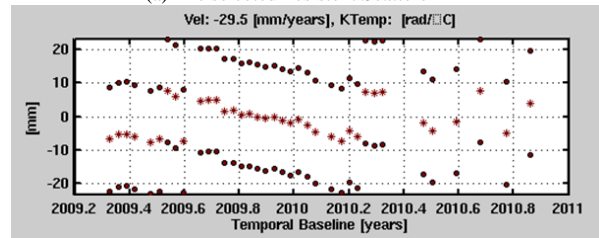
Figure 6. The geocoded Persistent Scatterer

X-band PS analysis was applied in one of the potential deformation area detected by L-band. The analyzed area is relatively small, about 15 by 10 sqkm (15350 by 6000 pixels). It is interesting to observe also in this case the MST graph connecting the available images shown in Figure 4 Left. We can in fact notice that the most coherent connections are mainly vertical, and this means with small temporal baselines. A possible reason of this behavior is the

strong motion affecting the ground (whenever the time distance is long, the phase of the interferograms decorrelate). At the same time, another possible explanation relates to the management of fields in the Tianjin area: it is in fact common in this region to cover cultivated plants with a structure for protecting them from bad weather conditions. This kind of changes of the ground surface makes it complex to interpret the spatial coherence and causes the failure of common models of the spatio/temporal behavior of the InSAR phase. Moreover, from Figure 4 we can notice, as a general comment, that we have a set of coherent images between the end of 2009 and the beginning of 2010 (yellow-red color), while much worse performances are registered at the beginning and at the end of our dataset (light blue color). We also observe that from spring 2010 we have less data separated by longer temporal baselines, making it more difficult to precisely estimate and reconstruct motion time series of PSs. Starting from the above considerations, we decided to process the area of interest with a common PS approach, using a star graph with a common master image as Figure 4 Right.



(a) The selected Persistent Scatterer P1



(b) The motion history of P1

Figure 7. The motion history of one selected Persistent Scatterer

Figure 5 shows the result of the linear deformation trend in geographical coordinates, after resampling on a regular grid. The colorbar in Figure 5 is given in mm/year, spanning values from -80 to 0. The deformation of the selected reference point is set to 0, and all analyzed PSs show a relative motion with respect to it. The area with strong subsidence rate can be easily recognized in yellow-red color, in good agreement with the signal found in the L band interferogram (Figure 3(a)). Figure 6 displays a snapshot of Google Earth with the geocoded PSs. The color shows the linear deformation trend of PSs with the same color scale as Figure 5. By clicking on the visualized points in Google

Earth one can read the deformation trend and the height of the corresponding PS. Figure 6 shows the actual density of the detected PSs.

Finally, in Figure 7 we report an example of time series of a given PS. The time series is plotted together with the ambiguous replica of the signal at half the wavelength. It is interesting to notice the deviations from the linear trend that deserve further investigation. It is also worth to point out again that the longer time distance between TSX acquisitions after spring 2010 makes it more difficult to estimate the real displacement.

4. CONCLUSION AND PERSPECTIVE

In this paper we report the INSAR time series analysis results for subsidence monitoring in Tianjin, where we experimented a new combination of L and X band that can be fruitfully used to draw a global acquisition planning for satellites like TSX, with high potentiality but not global coverage. Firstly, areas with evident motion are extracted from L band interferograms. Consequently, PS analyses are carried out on small areas corresponding to the motion observed in L band. As expected, deformation is confirmed by the X band analysis, with considerable amount of detail given by the high spatial and temporal resolution of TSX. The experiment demonstrates that it is possible to take advantage of pairs of ALOS images to make a first assessment of areas affected by strong motion and focus the X-band analysis. The research can provide a possible solution and reliable reference for wide area subsidence monitoring by INSAR time series analysis. Besides, the results of X-band PS analysis provide a proof that X-band has strong potential ability to be applied for monitoring infrastructures such as single building, and highway. For perspective, L-band PS analysis should be realized. The cross validation results between L-band and X-band will provide more meaningful guidance for subsidence monitoring. Moreover, Continuous monitoring with L band with longer time intervals will be able to update/modify the monitoring strategy with X-band. Meanwhile, when GPS data is available, quantitative comparison results can be acquired.

5. ACKNOWLEDGMENT

TerraSAR-X data are provided by Infoterra, Germany, while ALOS L-band data are provided by Japanese Earth Remote Sensing Data Analysis Center(ERSDAC). The software we used in this work is SARProz, developed by Daniele Perissin. The authors are very thankful to the partially support of the Research Grants Council of HKSAR (Ref. No.450210) and the project name is an integrated model for monitoring Qinghai-Tibet railway deformation based on DInSAR technology and GPS observations.

6. REFERENCES

- [1] Jie, Z. and H. Guang-dao, "Review on Land Subsidence Monitoring by InSAR," *Geological Science and Technology Information*, 2005.
- [2] Perissin, D. and T. Wang, "Time-Series InSAR Applications over Urban Areas in China," *Selected Topics in Applied Earth Observations and Remote Sensing, IEEE Journal of*, 2010(99): p. 1-9.
- [3] Qu, S., H. Yue, and W. Hong, "The analysis of permanent scatterers and its application in urban surface deformation monitoring of Tianjin," *IEEE*, 2008.
- [4] Perissin, D., A. Parizzi, and C. Rocca, "Monitoring Tianjin subsidence with the Permanent Scatterers technique," *Proceedings of the 2005 Dragon Symposium (SP-611)*, 27 June - 1 July 2005.
- [5] Baldi, P., et al., "GPS-based monitoring of land subsidence in the Po Plain (Northern Italy)," *Earth and Planetary Science Letters*, 2009. 288(1-2): p. 204-212.
- [6] Bitelli, G., F. Bonsignore, and M.Y. Unguendoli, "Levelling and GPS networks to monitor ground subsidence in the Southern Po Valley," *Journal of Geodynamics*, 2000. 30(3): p. 355-369.
- [7] Herring, T., "Geodetic applications of GPS," *Proceedings of the IEEE*, 2002. 87(1): p. 92-110.
- [8] Battaglia, M., et al., "Evidence for fluid migration as the source of deformation at Campi Flegrei caldera (Italy)," *Geophys. Res. Lett.*, 2006. 33.
- [9] Rott, H., "Advances in interferometric synthetic aperture radar (InSAR) in earth system science," *Progress in Physical Geography*, 2009. 33(6): p. 769-791.
- [10] Raucoules, D., C. Colesanti, and C. Carnec, "Use of SAR interferometry for detecting and assessing ground subsidence," *Comptes Rendus Geoscience*, 2007. 339(5): p. 289-302.
- [11] Ferretti, A., C. Prati, and F. Rocca, "Permanent scatterers in SAR interferometry," *Geoscience and Remote Sensing, IEEE Transactions on*, 2002. 39(1): p. 8-20.
- [12] Ferretti, A., C. Prati, and F. Rocca, "Nonlinear subsidence rate estimation using permanent scatterers in differential SAR interferometry," *Geoscience and Remote Sensing, IEEE Transactions on*, 2002. 38(5): p. 2202-2212.
- [13] Chaabouni-Chouayakh, H. and M. Datcu, "Coarse-to-Fine Approach for Urban Area Interpretation Using TerraSAR-X Data," *Ieee Geoscience and Remote Sensing Letters*. 7(1): p. 78-82.
- [14] Kim, D.J., W.M. Moon, and Y.S. Kim, "Application of TerraSAR-X Data for Emergent Oil-Spill Monitoring," *IEEE Transactions on Geoscience and Remote Sensing*, 2010. 48(2): p. 852-863.
- [15] D. Perissin, F. Rocca, "Landslide in Dossena (BG): comparison between interferometric techniques," *BIOGEOSAR* 25-28 September 2007.
- [16] Berardino, P., et al, "A two-scale differential SAR interferometry approach for investigating earth surface deformations," 2003: *IEEE*.
- [17] Berardino, P., et al., "A new algorithm for surface deformation monitoring based on small baseline differential SAR interferograms," *Geoscience and Remote Sensing, IEEE Transactions on*, 2002. 40(11): p. 2375-2383.
- [18] http://ihome.cuhk.edu.hk/~b122066/index_files/download.htm.